Abdelmadjid MENAD[1], Ali TAHRI[1]

Département d'électrotechnique, Faculté de Génie Electrique
Université des Sciences et de la Technologie d'Oran Mohamed Boudiaf -USTOMB -BP 1505 El Mnaouer -ORAN – ALGERIE (1)

doi:10.15199/48.2021.06.20

Experimental evaluation of a digital speed regulation of a PMDC motor by an HCS12 microcontroller

Abstract. *Rotating machines such as DC motors have wide use in industry. Generally permanent magnet direct current motors in various applications have good performance and simple control. This article describes a practical embodiment of a digital speed control implementation of a permanent magnet direct current motor with a PI regulator using a Motorola model HCS12 microcontroller. The latter receives the speed reference and generates the control signal (PWM) in order to control the armature voltage of the motor to satisfy the speed reference. The experimental results are given in this article.*

Streszczenie. *Generalnie silniki prądu stałego z magnesami trwałymi w różnych zastosowaniach mają dobrą wydajność i proste sterowanie. W tym artykule opisano praktyczną realizację implementacji cyfrowej regulacji prędkości silnika prądu stałego z magnesami trwałymi z regulatorem PI przy użyciu mikrokontrolera Motorola HCS12. Kontroler odbiera prędkość odniesienia i generuje sygnał sterujący (PWM) w celu sterowania napięciem twornika silnika w celu spełnienia zadanej prędkości. Wyniki eksperymentów podano w tym artykule. (**Eksperymentalna ocena cyfrowej regulacji prędkości silnika PMDC przez mikrokontroler HCS12*)

Keywords: DC motor with permanent magnets, identification of the mathematical model, HCS12 microcontroller, duty cycle, PI regulator.
Słowa kluczowe: Silnik prądu stałego z magnesami trwałymi, identyfikacja modelu matematycznego, mikrokontroler HCS12,.

Introduction

The contribution of digital regulation of a direct current motor for an experimental implementation is considerable. Numerous models are thus produced which allow a wide variety of constraints to be met: position regulation, speed regulation, motor protection.

The prescription of an experimental regulation results from a preliminary knowledge of the mathematical model of the regulated engine. An unknown motor parameter deficit is therefore prohibitive at this stage in order to achieve good regulation; for that we could use classical methods for identifications. But some of these methods might be less reliable. A simulation tool under MatLab would therefore be very useful here. It would also find an application space as a validation aid for the practical part.

It is in this general context that our work is situated. Where we present tools for analyzing and testing the procedure performed which allow:

- Identification of the parameters of the permanent magnet DC motor.
- To calculate the parameters of the PI regulator.
- Implemented the regulation program in the HCS12 microcontroller.
- Realized protection, against overcurrent, overvoltage, and speeding.
- Performs the series chopper (step down chopper) and carry out tests.

The method adopted for experimental regulation is to model the motor and make an appearing with the real response and simulate. This method is descriptive in the sense that we will seek to better choose the parameters of the PI regulator which will be well suited to the motor. The major difficulty is the actual capture of the speed in digital form and the correct flowchart implemented in the HCS12 microcontroller.

In this article we will first present the method used to identify the mathematical model of a permanent magnet direct current motor. Calculates controller parameters. Realization of the different experimental parts. And we end with experimental and discussed results.

The engione speed control system

The overall operating diagram of the speed control system used in the embodiment is given in Fig. 1.

The complete system consists of a rectifying and filtered DC voltage source, a step-down chopper, a permanent magnet DC motor connected to a driving wheel with a braking device for the variation of the resistive torque; a speed sensor, and a speed controller, generates the control signal to satisfy the given speed reference.

The chopper is used here as an interface device between the DC voltage source and the motor in order to have a controllable voltage across the motor at a desired speed.

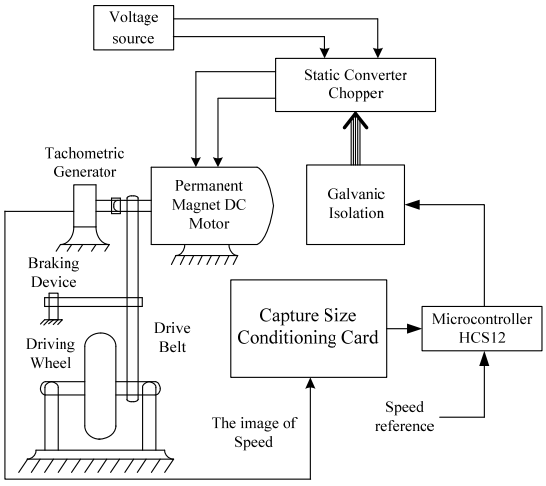

Fig.1 Block diagram of the system to be produced

Modeling of the direct current in a permanent magnet machine [1]

The following equations govern the dynamics of the engine:

$$v_a(t) = R_a i_a(t) + L_a \frac{d}{dt} i_a(t) + e(t) \quad (1)$$

$$e(t) = K_e \omega_r(t) \quad (2)$$

$$T_e(t) = K_t i_a(t) \quad (3)$$

$$J \frac{d}{dt} \omega_r(t) + f \omega_r(t) = T_e(t) + T_l(t) \quad (4)$$

Using Laplace's theorem, the transformation of the two equations (1) and (4) constitutes the functional model represented in Fig. 2.

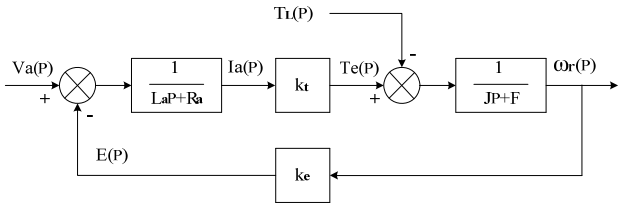

Fig. 2 Functional model of the armature control of a permanent magnet direct current motor

The standard form of the transfer function of such a second-order system is as follows:

(5) $$G_{\omega}(P)=\frac{\frac{k_t}{JL_a}}{\left(P+\frac{R_a}{L_a}\right)\left(P+\frac{F}{J}\right)+\frac{k_e k_t}{JL_a}}=\frac{k_m\omega_n^2}{P^2+2\xi\omega_n P+\omega_n^2}$$

And also, to a clear form:

(6) $$G_{\omega}(P)=\frac{k_m\omega_n^2}{(P-P_1)(P-P_2)}=\frac{k_m\omega_n^2\tau_1\tau_2}{(\tau_1 P+1)(\tau_2 P+1)}$$

There where: $$\tau_1=-\frac{1}{P_1};\quad \tau_2=-\frac{1}{P_2}$$

The static converter [2]

The diagram of this static converter which is a voltage step-down is given by Fig. 3.

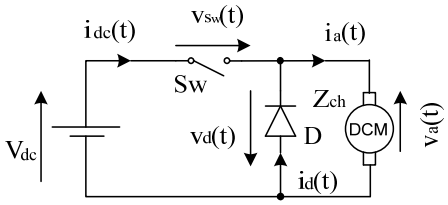

Fig 3 Block diagram of a series chopper

For a given duty cycle α, and in continuous conduction regime, the average voltage at the output is given by:

(7) $$V_a=\alpha V_{dc}$$

During the T_{ON} conduction period, the switch Sw is tripped, so that the voltage across the chopper is applied directly to the motor armature (see Fig. 3).

The T_{ON} is the conduction period of the switch Sw is determined by the controller which generates the required pulse, and therefore the duty cycle of the chopper α will be determined as follows:

(8) $$\alpha=\frac{T_{on}}{T_{max}}$$

Which give:

(9) $$T_{on}=\alpha T_{max}$$

Where T_{MAX} is the maximum period of the hash constant

Identification of the mathematical model of the machine

There are a large number of identification methods, among the most used parametric methods, we have the Broïda method. [3]

The solution consists in calculating 40% and 28% of the gain, then in recording the times proportional to the values of these gains to determine the unknowns in the transfer function given by the following equation:

(10) $$G(P)=\frac{k.e^{-rP}}{1+\tau P}$$

With: r : system startup delay; τ : system time constant; K : system gain.

(11) $$r=5,5.(t_{40\%}-t_{28\%})$$

(12) $$\tau=2,8.t_{28\%}-1,87.t_{40\%}$$

We approximate the engine start delay using the equation:

(13) $$e^{-rP}\cong\frac{1}{1+r.P}$$

So, equation (10) will be approximated as follows:

(14) $$G(P)=\frac{k}{(1+\tau.P)(1+r.P)}$$

So, the poles are: $$P_1=\frac{-1}{\tau}\quad;\quad P_2=\frac{-1}{r}$$

We injected a step at the input of the chopper, in order to supply the motor with a PWM control with 99% duty cycle and 1kHz frequency, and we observed and captured the evolution of the speed curve below (see Fig 4).

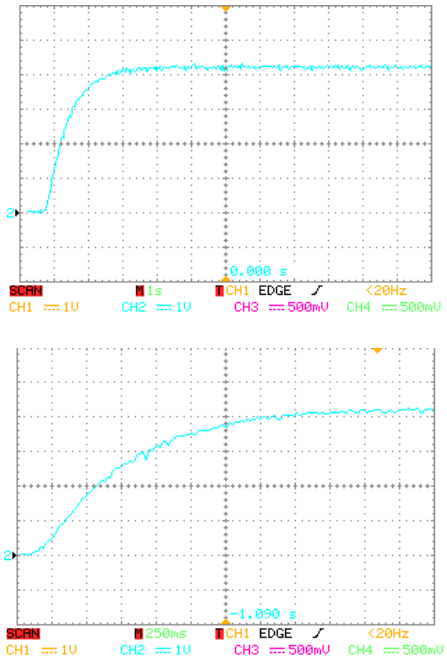

Fig 4 Response to a voltage step

The final value of the speed image is:

(15) $$v_N=4,2.1=4,2V\Rightarrow N=\frac{v_N}{K_{GC}}=\frac{4,2}{0,002}=2100tr/min$$

(16) $$k_{GC}=k_G.k_C=\frac{1}{1000}.2=0,002$$

k_G: gain of the tachometric generator; k_C: gain in conditioning the speed image.

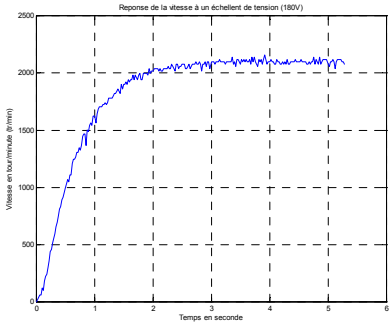

Fig. 5 The speed image modulated in MatLab

With identification and application of the Broida method to response taken from the machine speed (see Fig. 4), the system is as follows:

(17) $$G(P)=\frac{4.2}{(1+0,09696.P)(1+0,5819.P)}$$

Determining the mathematical model of the motor gives the possibility of comparing the speed response under MatLab (see Fig. 5), and that to be achieved in practice (see Fig. 4); which are almost identical.

Integral proportional regulation [4]

The transfer function of a classic PI regulator is given by the following relation:

(18) $$C(P)=\frac{U(P)}{E(P)}=K_p\left(1+\frac{1}{T_i.P}\right)=K_p+\frac{K_i}{P}=\frac{K_p.P+K_i}{P}$$

A. Identification of PI regulator parameters

The setting of the parameters of the PI regulator is carried out by different methods; among them, there is a simpler one, it is the Méplat criterion, and is applied as follows:

Open Loop system:

(19) $$G_{co}(P)=G(P).C(P)=\frac{K}{(1+\tau_1.P)(1+\tau_2.P)}.K_p\frac{(1+T_i.P)}{T_i.P}$$

The Méplat criterion consists of compensating for the dominant pole by choosing the integral time as follows:

$$T_i=\tau_{max} \overset{applied}{\Rightarrow} T_i=\tau_2=0,5819\,sec$$

And the equation of the open loop system becomes as follows:

(20) $$G_{co}(P)=G(P).C(P)=\frac{K.K_p}{T_i.P.(1+\tau_1.P)}$$

Close Loop system:

$$G_{cf}(P)=\frac{G_{co(P)}}{1+G_{co(P)}}=\frac{\frac{K.K_p}{\tau_1.\tau_2.P^2+\tau_2.P}}{1+\frac{KK_p}{\tau_1.\tau_2.P^2+\tau_2.P}}$$

And the transfer function written in the form of a second order system:

(21) $$G_{cf}(P)=\frac{\left(\frac{K.K_p}{\tau_1.\tau_2}\right)}{P^2+\frac{1}{\tau_1}.P+\left(\frac{K.K_p}{\tau_1.\tau_2}\right)}=\frac{\omega_n^2}{P^2+2\xi\omega_n P+\omega_n^2}$$

So, we have:

$$\omega_n=\sqrt{\frac{K.K_p}{\tau_1.\tau_2}}$$

$$2\xi\omega_n=\frac{1}{\tau_1} \Rightarrow \xi=\frac{1}{2\tau_1\omega_n}=\frac{1}{2\tau_1\sqrt{\frac{K.K_p}{\tau_1.\tau_2}}}$$

$$K_p=\frac{\tau_2}{4.K.\xi^2.\tau_1}=\frac{T_i}{4.K.\xi^2.\tau_1}$$

Let us choose as criteria:

- A zero-static error.
- An overrun of less than 5%.
- A settling time of 2% or less than 2.3 seconds.

$$D_p=100.exp\left(\frac{-\pi\xi}{\sqrt{1-\xi^2}}\right)=5\% \overset{by\ calculation\ we\ find}{\Rightarrow} \xi=0,6906$$

$$\begin{cases} Si:\xi\to 0\Rightarrow D_p\to 100\% \overset{overrun\ less\ than\ 5\%}{\Rightarrow} 0,6906<\xi<1 \overset{as\ a\ choice}{\Rightarrow} \xi=0,707 \\ Et\,si:\xi\to 1\Rightarrow D_p\to 0\% \end{cases}$$

$$\xi=0,707\Rightarrow D_p=4,325\%$$

$$K_p=\frac{T_i}{4.K.\xi^2.\tau_1}=\frac{0,5819}{4.4,2.0,707^2.0,09696}=0,7146$$

$$K_i=\frac{K_p}{T_i}=\frac{0,7146}{0,5819}=1,228$$

To be able to implement this regulation in a digital computer, it is essential to discretize it.

B. Choice of sampling step

This sampling period Ts must be chosen according to the system dynamics, by supporting Shannon's theorem (sampling theorem): [5]

(22) $$5.F_c<\frac{1}{T_s}<25.F_c$$

Fc: Cutoff frequency of the regulated system.

According to the motor model of equation (17), the cutoff frequency is as follows:

$$\omega_n=4,21rad/sec\Rightarrow\begin{cases} f_c=\frac{\omega_n}{2\pi}\Rightarrow f_c=0,67Hz \\ T_c=\frac{1}{f_c}\Rightarrow T_c=1,4925sec \end{cases}$$

$$3,35Hz<\frac{1}{T_s}<16,75Hz \Leftrightarrow 59,7msec<T_s<298,5msec$$

Our choice fell on: $T_s=60msec$.

C. Synthesis of the discretization of the PI regulator

The transition from a continuous system to a discrete system must be done by an approximation of the variable "P".

The chosen approximation and that of Tustin (bilinear or trapezoidal):

(23) $$P=\frac{2}{T_s}.\frac{z-1}{z+1}$$

Ts: the sampling time.

If we replace the Laplace variable by its equivalent in the numerical domain we find:

(24) $$C(P)=\frac{U(P)}{E(P)}=K_p\left(1+\frac{1}{T_i.P}\right)$$

(25) $$C(z)=K_p\left(1+\frac{1}{T_i.\frac{2(z-1)}{T_s(z+1)}}\right)$$

The recurrent equation of the corrector is given as follows:

(26) $$U(n)=A.E(n)+B.E(n-1)+U(n-1)$$

and:

$$A=K_p\left(1+\frac{T_s}{2T_i}\right)\Rightarrow A=0,7146\left(1+\frac{60.10^{-3}}{2.0,5819}\right)\Rightarrow A=0,7514$$

$$B=K_p\left(\frac{T_s}{2T_i}-1\right)\Rightarrow B=0,7146\left(\frac{60.10^{-3}}{2.0,5819}-1\right)\Rightarrow B=-0,6777$$

Reralization of the speed regulation chain

a. Speed setpoint

The speed reference is given by voltage variation delivered by a potentiometer between 0Volts and 5Volts.

b. Speed sensor [6]

Fig. 7 shows the circuit for conditioning the speed measurement so that it is ready for use by the microcontroller. And as conditioning we have:

- Speed sensor (the generator) with a differential amplifier (Part A).
- Active unity gain filter (Part B).
- Gain adjustment (Part C).
- Impedance adaptation (Part D).
-

Fig. 6 Image of the tachometer used

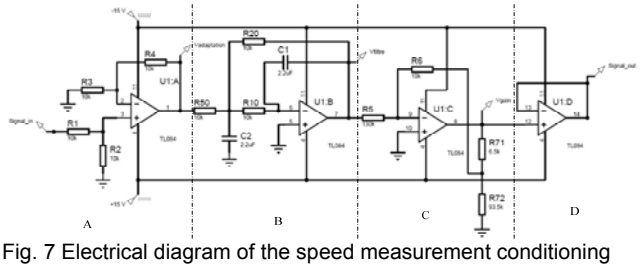

Fig. 7 Electrical diagram of the speed measurement conditioning

c. Voltage sensor and current sensor [6]

The two sensors have the same packaging chain; for the voltage (see Fig. 8), and the current (see Fig. 9).

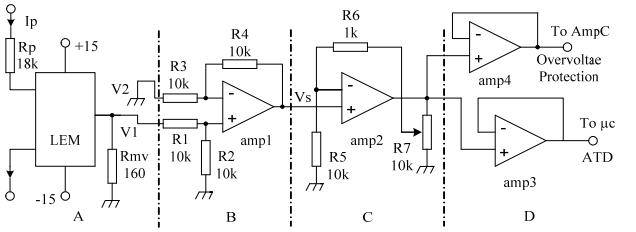

Fig. 8 Electrical diagram of the voltage measurement conditioning

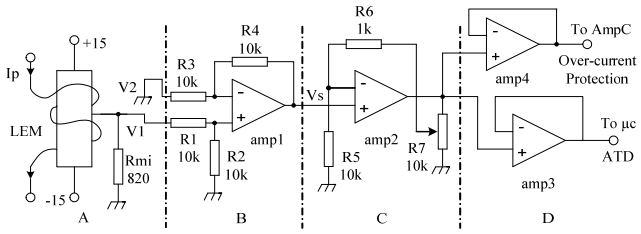

Fig. 9 Electrical diagram of the current measurement conditioning

The difference between the two sensors is in part (A) of the LEM hall effect element:

- LEM current sensor, LA 55P.
- LEM voltage sensor, LV 25P.

And as conditioning we have:

- Voltage or current sensor (Part A).
- Differential amplifier (Part B).
- Gain adjustment (Part C).
- Impedance adaptation (Part D).

d. Implementation of the regulator in the HCS12 microcontroller [7]

The program flow chart in Fig. 10, shows the flow of the regulation program in the microcontroller.

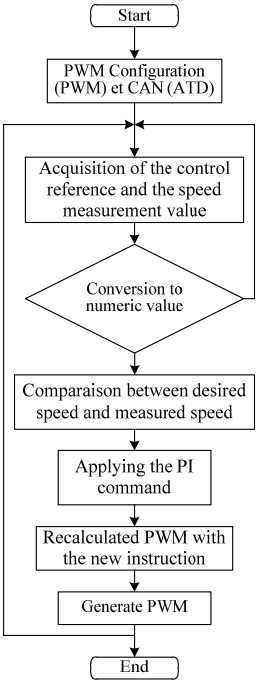

Fig. 10 The flowchart of the PI command implemented in the HCS12 microcontroller

e. Power circuit (Chopper)

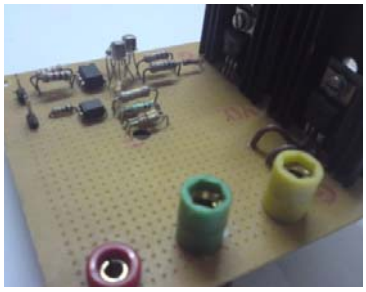

Fig. 11 Photo of the power part produced

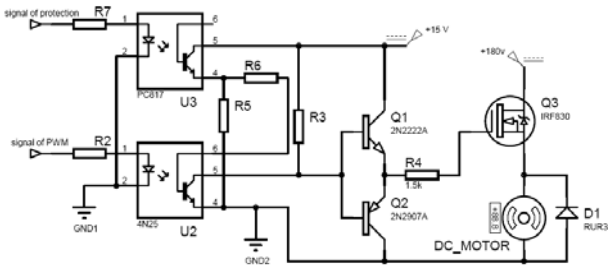

Fig. 12 Electrical diagram of the power section

Fig. 11 shows the different parts of the power circuit where we can find:

- Galvanic isolation
- The attack circuit floor.
- The motor control IGBT with the voltage source

f. The motorization of the permanent magnet motor with direct current

g. Fig. 13 sheds light on the idea of mounting the motor, consists of an engine, a tacho-generator and a wheel connected with a belt brake by another small wheel which pulls the belt down as a resistant torque.

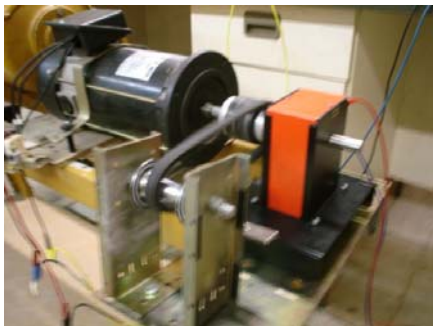

Fig. 13 Image of the motorization used

Electric motor characteristics:
180 Volts; 4.9 Amps; 1750 rpm

g. Galvanic isolation and protection

Galvanic isolation:

Galvanic isolation is achieved by the 4N25 and PC817 optocoupler between the power part and the control part, ensuring isolation and separation of the masses in the event of a short circuit, the control part remains protected.

Protection of the HCS12 µc data acquisition converter (ATD): [8]

At the input of each pin of the converter, we use a small assembly based on two Schottky diodes and a resistor, as clear protection in Fig. 14.

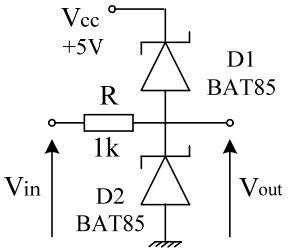

Fig. 14 Electrical diagram of ATD converter protection

Voltage and current protection:

In the interest of good protection of our motor, we have installed protections against overcurrent and overvoltage generated by control or handling faults.

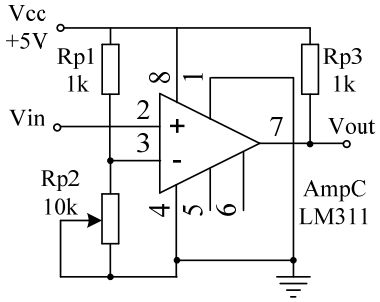

Fig. 15 Diagram of overvoltage and overcurrent protection

Fig. 15 presents a LM311 based comparator, either in voltage or current in the same assembly, monitors the measured value (voltage or current) and compares it with the value chosen as limit through the potentiometer Rp2.

The protection of our control chain (see Fig. 16) is based on the measurement delivered by the two voltage and current sensors, to block the optocouplers (4N25) and cause the blocking of the transistor (Q3: IRF830), thus the total stop of the chopper.

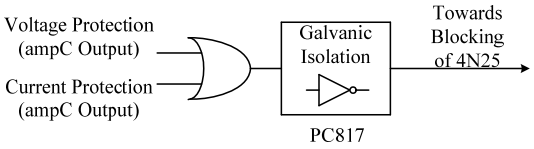

Fig. 16 Block diagram of the protection

Experimental results

a. Protection circuit test

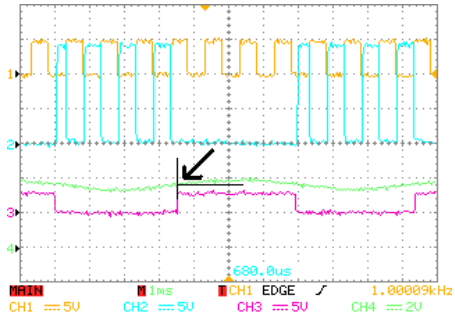

Fig. 17 Testing overcurrent protection

After testing the current protection (see Fig. 17), we noticed that when the current (Channel 4) exceeds its chosen protection reference (see arrow in Fig. 17), the protection circuit generates a voltage at the input of the PC817 optocoupler (Channel 3) to block the MOSFET driver circuit, cancel its control voltage (Channel 2); which will cause the power circuit to shut down, even though the PWM at the input of the 4N25 optocoupler (Channel 1) exists.

b. Closed Loop PI Control Test

After testing the control chain of our prototype, we implemented the PI regulator algorithm in the HCS12 microcontroller, and we wired the assembly.

The following synoptic diagram (see Fig. 18) clearly shows the progress of the regulation chain.

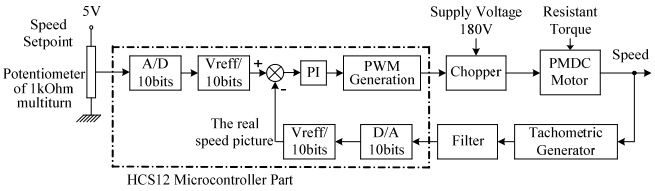

Fig. 18 Block diagram of the different states of the PI regulation

c. Test with constant loads

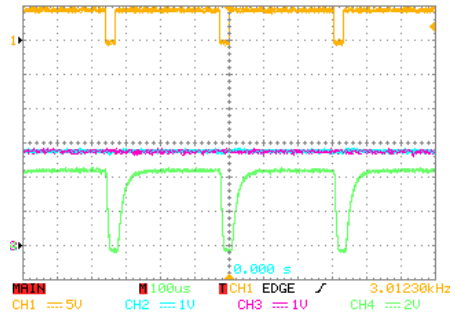

CH1: PWM-CH2: MEASUREMENT (N)
CH3: SETPOINT (N) -CH4: VOLTAGE

Fig. 19.a Results of the PI regulator on load (VC=2.8V, N=1860tr/min)

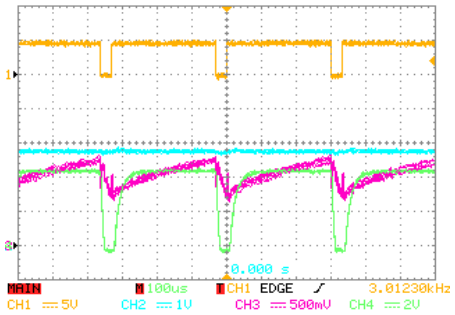

CH1: PWM-CH2: MEASURE (N)
CH3: MEASURE (Ia) -CH4: VOLTAGE

Fig. 19.b Results of the PI regulator on load. (Ia = 1A)

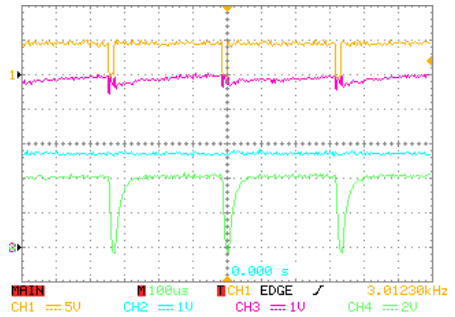

CH1: PWM-CH2: MEASURE (N)
CH3: MEASURE (Ia) -CH4: VOLTAGE

Fig. 19.c Results of the PI regulator under load. (Ia = 5A)

d. Test with varying loads

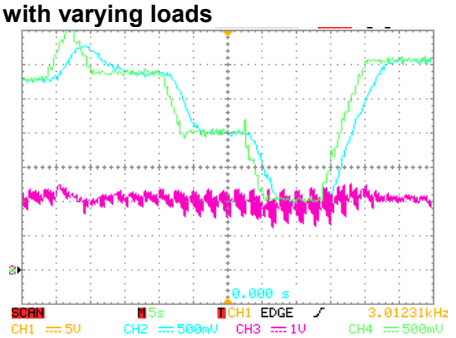

CH2: MEASUREMENT (N) -CH3: MEASUREMENT (Ia)
CH4: SETPOINT (N)

Fig. 20 Speed response with the PI regulator on load. (Ia ≈ 2.4A)

The results shown in Fig. 19.a confirm the speed regulation (Channel 2) with respect to its reference (Channel 3) with a low load (translated by the value of the current (Channel 3 in Fig. 19.b).

Note in the different Fig. 19.b to Fig. 19.c, that the variation of the load implies the variation of the current and we have reached the nominal speed of the machine, with a constant speed by the implemented regulator.

We can also notice in Fig. 19 the slight variation of the PWM (Channel 1) with that of the voltage (Channel 3) to keep the speed constant following the variation of the load.

With a variable load, the PI regulator has given good results where it can be seen in Fig. 20 that the measured speed (Channel 2) follows its setpoint (Channel 4) with a slight delay of almost 2 seconds.

Conclusion

The Closed Loop Adjustable DC Motor Speed control system is based on the identification of the mathematical model of the motor and the use of a microcontroller.

The training process begins with an identification of the mathematical model of the motor, after which it was possible to define the parameters of the PI controller, which are implemented in the HCS12 microcontroller.

This system is applicable to different sizes of motors and of course the limited power of the Chopper is taken into account.

In addition, the over-voltage and over-current protection system gave an appreciable response.

Thus, it can be concluded that the current system under study is a reliable adjustable drive system for permanent magnet direct current motors, without or with the parameters of the latter.

***Authors**: dr Abdelmadjid Menad, faculty electrical engineering electrical department, University of Science and Technology Oran Mohamed-Boudiaf – El Mnaouar, BP 1505, Bir El Djir 31000, Oran, ALGERIA, E-mail: abmenad@gmail.com; Prof Ali Tahri, faculty electrical engineering electrical department, University of Science and Technology Oran Mohamed-Boudiaf – El Mnaouar, BP 1505, Bir El Djir 31000, Oran, ALGERIA, E-mail: alitahri@gmail.com.*

REFERENCES

[1] P. Krause, O. Wasynczuk, S. Sudhoff, S. Pekarek, “Analysis of Electric Machinery and Drive Systems”, Third Edition, IEEE PRESS, 2013

[2] M. H. Rashid, “Power Electronics” Prentice-Hall International Edition, 1988

[3] J.M. Flous, ‘La régulation industrielle’, édition Hernés, 1994.

[4] R. Longchamp, ‘Commande numérique de systèmes dynamiques’, édition Technique et Documentation (Lavoisir), 1995

[5] Roland S. Burns, “Advanced Control Engineering” Butterworth-Heinemann Edition, 2001

[6] B. Haraouibia, ‘Les amplificateurs operationnels, fonctionement et application ‘, les carnets de l’ingenieur, édition ENAG.

[7] ‘MC9S12DP512 Device Guide V01.25’, Motorola, Inc, Revised 05 Jul 2005.

[8] R. G. Seippel, ‘Tranducer Interfacing, Signal conditioning for Process Control’, Prentice-Hall, Inc, Enlewoad Cliffs, New Jersey, 1988.